CHAPTER III

THEORY

3.1 Structure of Zeolites

Zeolites are porous, crystalline aluminosilicates that develop uniform pore structure having minimum channel diameter of 0.3 to 1.0 nm. This size depends primarily upon the type of zeolite. Zeolites provide high activity and unusual selectivity in a variety of acid-catalyzed reactions. Most of the reactions are caused by the acidic nature of zeolites.

The structure of zeolites consists of a three-dimentional framework of SiO_4 or AlO_4 tetrahedra, each of which contains a silicon or aluminum atom in the center. The oxygen atoms are shared between adjoining tetrahedra, which can be present in various ratios and arranged in a variety of ways. The framework thus obtained contains pores, channels, and cages, or interconnected voids.

Zeolites may be represented by the general formular,

$$M_{x/n}[(AlO_2)_x(SiO_2)_y]wH_2O$$

where the term in brackets is the crystallographic unit cell. The metal cation of valence *n* is present to produce electrical

neutrality since for each aluminum tetrahedron in the lattice there is an overall charge of -1 [58]. M is a proton, the zeolite becomes a strong Bronsted acid. As catalysts, zeolites are unique in their ability to discriminate between reactant molecules and to control product selectivity, depending on molecular size and shape [60].

The catalytically most significant zeolites are those having pore openings characterized by 8-, 10-, and 12- rings of oxygen atoms. Some typical pore geometries are shown in Figure 3.1 [59].

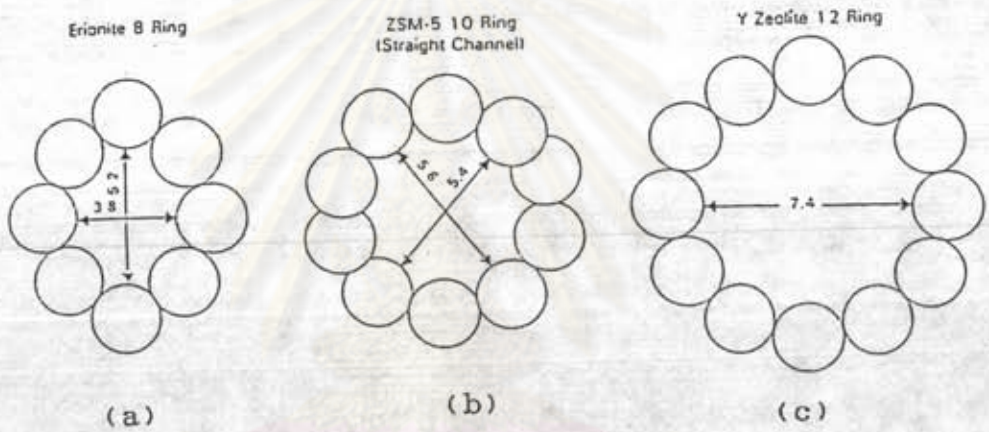

Figure 3.1 Typical zeolite pore geometries [59].

The framework of zeolites used most frequently as adsorbent or catalyst are shown in Figures 3.2-3.5. The Al or Si atoms are located at the intersection of lines that represent oxygen bridges. The X and Y zeolites are structually and topologically related to the mineral faujasite and frequently refered to as faujasite-type zeolites. The two materials differ chemically by their Si/Al ratios, which are 1-1.5 and 1.5-3.0 for X and Y zeolite, respectively. In faujasites, large cavities of 1.3 nm in diameter (supercages) are connected to each other

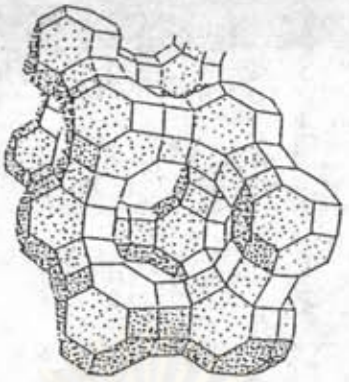

Figure 3.2 Structure of type-Y (or X) zeolite [58].

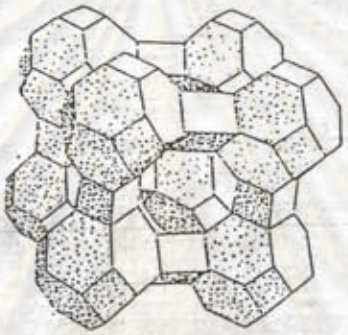

Figure 3.3 Structure of type-A zeolite [58].

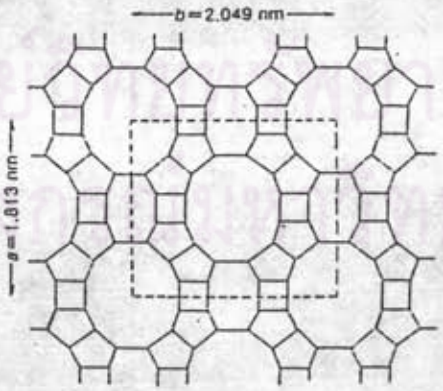

Figure 3.4 Skeletal diagram of the (001) face of mordenite [58].

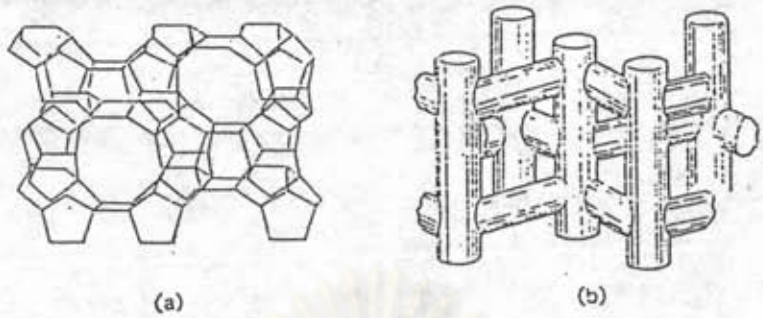

Figure 3.5 Structure of ZSM-5 (a) Skeletal diagram of the (010) face of ZSM-5 (b) channel network [58].

through apertures of 1.0 nm.

In type A zeolite (Figure 3.3), large cavities are connected through apertures of 0.5 nm, determined by eight-membered rings (Figure 3.1a).

The mordenite pore structure (Figure 3.4) consists of elliptical and noninterconnected channels parallel to the *c*-axis of the orthorhombic structure. Their openings are limited by twelve-membered rings (0.6-0.7 nm) (Figure 3.1c). ZSM-5 zeolite (Figure 3.5) shows a unique pore structure that consists of two intersecting channel systems: one strainght and the other sinusoidal and perpendicular to the former (Figure 3.5). Both channel systems have ten-membered-rings elliptical openings (ca. 0.55 A in diameter) (Figure 3.1b) [58].

3.2 Acidity of Zeolite

Classical Bronsted and Lewis acid models of acidity have been used to classify the active sites on zeolites. Bronsted acidity is proton donor acidity; a trigonally coordinated alumina atom is an electron deficient and can accept an electron pair, therefore behaves as a Lewis acid [60,61].

In general, the increase in Si/Al ratio will increase acidic strength and thermal stability of zeolite [62]. Since the number of acidic OH groups depend on the number of aluminum in zeolite's framework, decrease in Al content is expected to reduce catalytic activity of zeolite. If the effect of increase in the acidic centers, decrease in Al content shall result in enhancement of catalytic activity.

Based on electrostatic consideration, the charge density at a cation site increases with increasing Si/Al ratio. It was conceived that these phenomena are related to reduction of electrostatic interaction between framework sites, and possibly to difference in the order of aluminum in zeolite crystal - the location of Al in crystal structure [61].

Recently it has been reported the mean charge on the proton was shifted regularly towards higher values as the Al content decreased [60]. Simultaneously the total number of acidic hydroxyls, governed by the Al atoms, were decreased. This evidence emphasized that the entire acid strength distribution (weak, medium, strong) was shifted towards stronger values. That is, weaker acid sites become stronger with the decrease in Al content.

An improvement in thermal or hydrothermal stability has been ascribed to the lower density of hydroxyls groups which parallel to that of Al content [58]. A longer distance between hydroxyl groups decreases the probability of dehydroxylation that generates defects on structure of zeolites.

3.3 Generation of Acid Centers

Protonic acid centers of zeolite are generated invarious ways. Figure 3.6 depicts the thermal decomposition of ammonium exchanged zeolites yielding the hydrogen form [63].

The Bronsted acidity due to water ionization on polyvalent cations, described below, is depicted in Figure 3.7 [58].

$$M^{n+} + xH_2O \longrightarrow M(OH)_x^{(n-x)+} + xH^+ \qquad (3.1)$$

The exchange of monovalent ions by polyvalent cations could improve the catalytic property. Those highly charged cations create very acidic centers by hydrolysis phenomena.

Bronsted acid sites are also generated by the reduction of transition metal cations. The concentration of OH groups of zeolite containing transition metals was noted to increase by reduction with hydrogen at 250-450 ^{o}C at to increase with the rise of the reduction temperature [63].

$$Cu^{2+} + H_2 \longrightarrow Cu^{o} + 2H^+ \qquad (3.2)$$

$$Ag^+ + 1/2\ H_2 \longrightarrow Ag^{o} + H^+ \qquad (3.3)$$

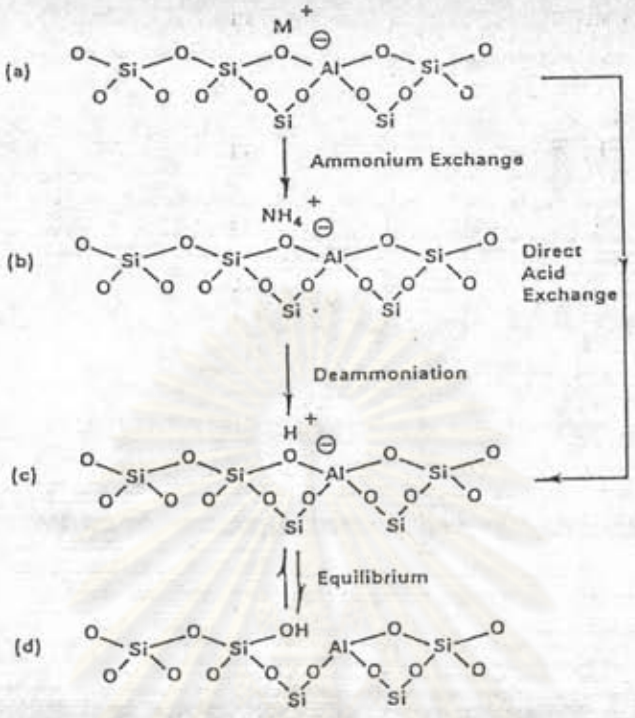

Figure 3.6 Diagram of the surface of a zeolite flamework [63].

a) In the as-synthesized form M^+ is either an organic cation or an alkalimetal cation.

b) Ammonium in exchange produces the NH_4^+ exchanged form.

c) Thermal treatment is used to remove ammonia, producing the H^+, acid, form.

d) The acid form in (c) is in equilibrium with the form shown in (d), where there is a silanol group adjacent to a tricoordinate aluminum.

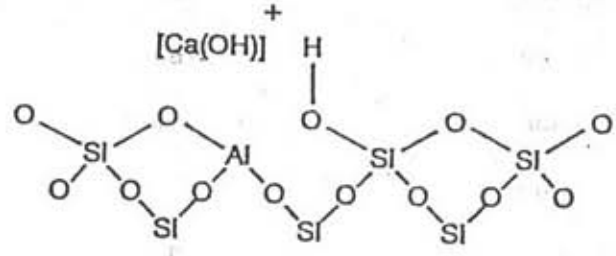

Figure 3.7 Water molecules coordinated to polyvalent cation are dissociated by heat treatment yielding Bronsted acidity [58].

The formation of Lewis acidity from Bronsted sites is depicted in Figure 3.8 [58]. The dehydration reaction decreases the number of protons and increases that of Lewis sites.

Bronsted (OH) and Lewis (-Al-) sites can be present simultaneously in the structure of zeolite at high temperature. Dehydroxylation is thought to occur in ZSM-5 zeolite above 500^{o}C and calcination at 800 to 900 ^{o}C produces irreversible dehydroxylation which causes defection in crystal structure of zeolite.

Dealumination is believed to occur during dehydroxylation which may result from the steam generation within the sample. The dealumination is indicated by an increase in the surface concentration of aluminum on the crystal. The dealumination process is expressed in Figure 3.9 [58]. The extent of dealumination monotonously increases with the partial pressure of steam.

The enhancement of the acid strength of OH groups is recently proposed to be pertinent to their interaction with those aluminum species sites are tentatively expressed in Figure 3.10 [58]. Partial dealumination might, therefore, yield a catalyst of higher

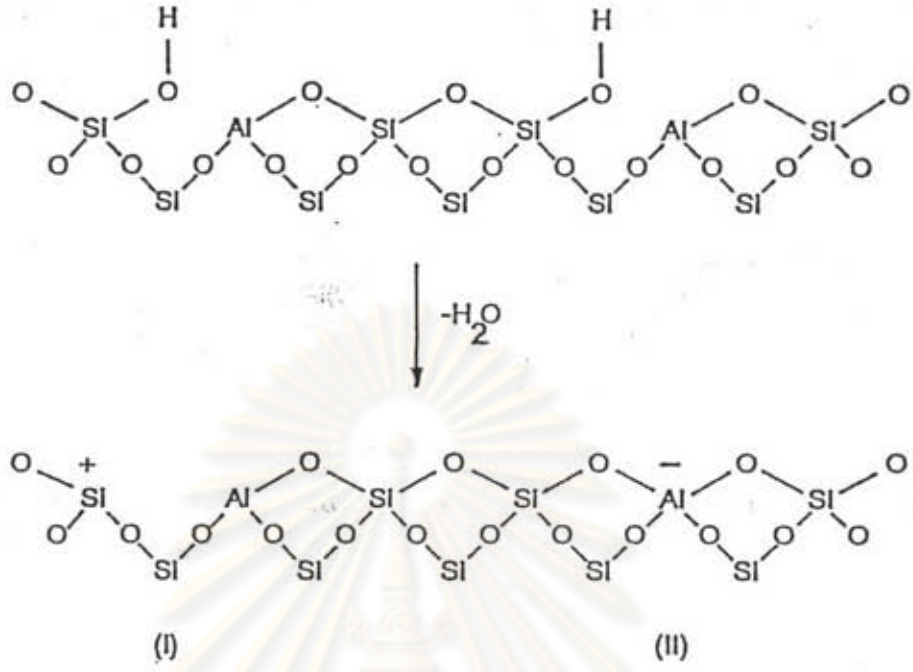

Figure 3.8 Lewis acid site developed by dehydroxylation of Bronsted acid site [58].

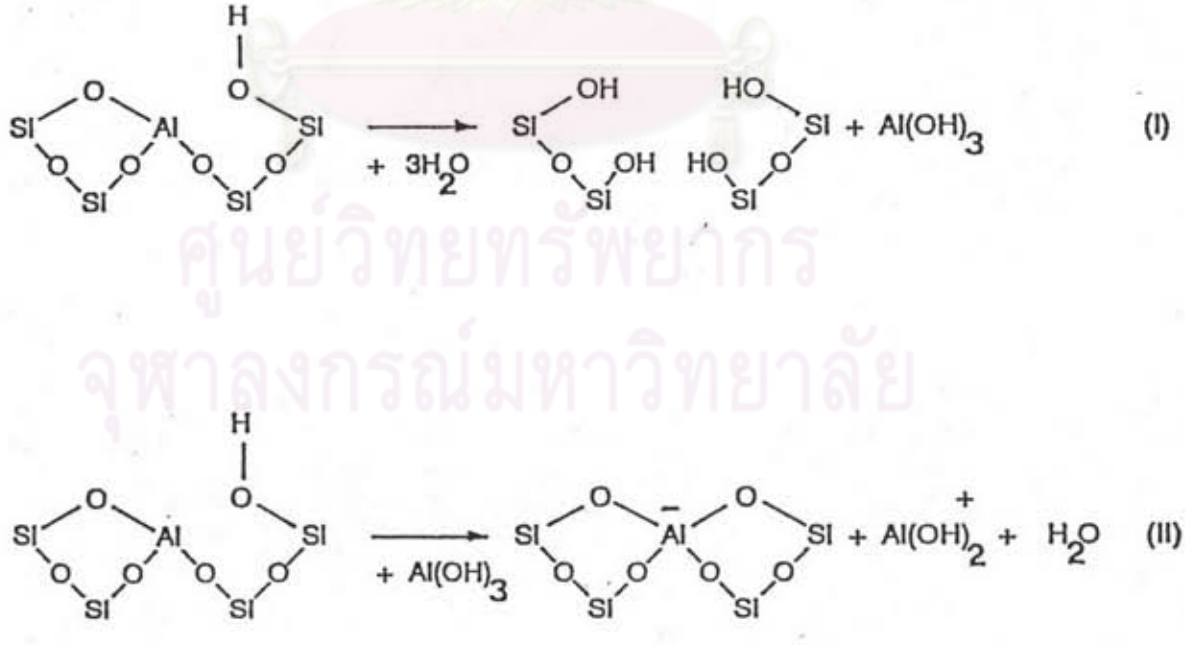

Figure 3.9 Steam dealumination process in zeolite [58].

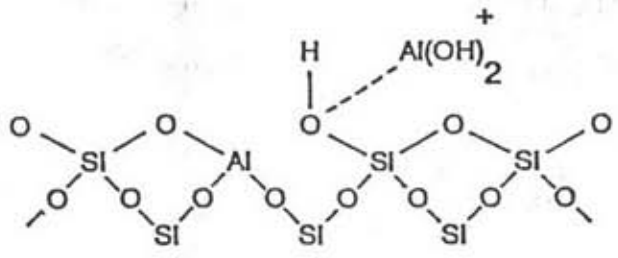

Figure 3.10 The enhancement of the acid strength of OH groups by their interaction with dislodged aluminum species [58].

activity while severe steaming reduces the catalytic activity.

3.4 Shape Selectivity

Many reactions involving carbonium ions intermediates are catalyzed by acidic zeolites. With respect to a chemical standpoint the reaction mechanisms are not fundamentally different with zeolites or with any other acidic oxides. What zeolite add is shape selectivity effect. The shape selective characteristics of zeolites influence their catalytic phenomena by three modes; reactants shape selectivity, products shape selectivity and transition states shape selectivity [63-65]. These type of selectivity are depicted in Figure 3.11.

Reactant or charge selectivity results from the limited diffusibility of some of reactants, which cannot effectively enter and diffuse inside crystal pore structures of the zeolites.

Product shape selectivity occurs as slowly diffusing product molecules cannot escape from the crystal and undergo secondary reactions.

a) Reactant selectivity

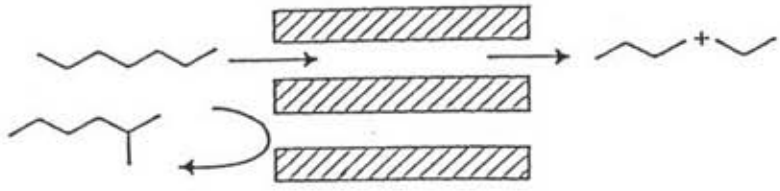

b) Product selectivity

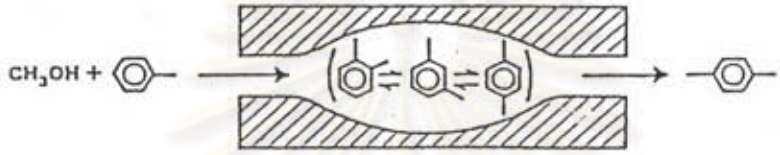

c) Transient state selectivity

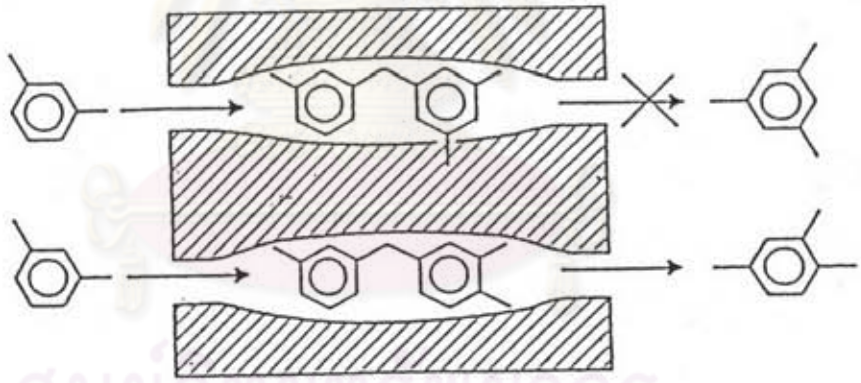

Figure 3.11 Diagram depicting the three type of selectivity [63].

Restricted transition state shape selectivity is a kinetic effect arising from local environment around the active site, the rate constant for a certain reaction mechanism is reduced if the space required for formation of necessary transition state is restricted.

The critical diameter (as opposed to the length) of the molecules and the pore channel diameter of zeolites are important in predicting shape selective effects. However, molecules are deformable and can pass through openings which are smaller than their critical diameters. Hence, not only size but also the dynamics and structure of the molecules must be taken into account.

Table 3.1 presents values of selected critical molecular diameters and Table 3.2 presents values of the effective pore size of various zeolites. Correlation between pore size(s) of zeolites and kinetic diameter of some molecules are depicted in Figure 3.12.

3.5 Reaction Mechanism of Methanol Conversion

The conversion of methanol over ZSM-5 zeolites was investigated by Chang and Silvestri [5]. The reaction can be proceeded to the following general reaction path:

$$2CH_3OH \underset{+H_2O}{\overset{-H_2O}{\rightleftharpoons}} CH_3OCH_3 \xrightarrow{-H_2O} C_2^{2-}\text{-}C_5^{2-} \longrightarrow \begin{matrix} \text{paraffins} \\ \text{aromatics} \\ \text{cycloparaffins} \\ C_6^{+}\ \text{olefins} \end{matrix}$$

Scheme A

Table 3.1 Kinetic diameters of various molecules based on the Lenard-Jones relationship [67].

	KINETIC DIAMETER (ANGSTROMS)
He	2.6
H_2	2.89
O_2	3.46
N_2	3.64
NO	3.17
CO	3.76
CO_2	3.3
H_2O	2.65
NH_3	2.6
CH_4	3.8
C_2H_2	3.3
C_2H_4	3.9
C_3H_8	4.3
$n\text{-}C_4H_{10}$	4.3
Cyclopropane	4.23
$i\text{-}C_4H_{10}$	5.0
$n\text{-}C_5H_{12}$	4.9
SF_6	5.5
Neopentane	6.2
$(C_4F_9)_3N$	10.2
Benzene	5.85
Cyclohexane	6.0
m-xylene	7.1
p-xylene	6.75
1,3,5 trimethylbenzene	8.5
1,3,5 triethylbenzene	9.2
1,3 diethylbenzene	7.4
1-methylnaphthalene	7.9
$(C_4H_9)_3N$	8.1

This reaction path is established by monitoring changes in product distribution as a function of varying contact time, shows in Figure 3.13. An essentially identical reaction path is obtained with DME as feed, Figure 3.14, confirming its intermediacy in the reaction sequence.

Table 3.2 Shape of the pore mouth openings of known zeolite structures. The dimensions are based on two parameters, the T atoms forming the chennel opening (8, 10, 12 rings) and the crystallographic free diameters of the channels. The channels are parallel to the crystallographic axis shown in brackets (e.g. <100>) [63].

STRUCTURE	8-MEMBER RING	10-MEMBER RING	12-MEMBER RING
Bikitaite	3.2×4.9[001]		
Brewsterite	2.3×5.0[100]		
	2.7×4.1[001]		
Cancrinite			6.2[001]
Chabazite	3.6×3.7[001]		
Dachiardite	3.6×4.8[001]	3.7×6.7[010]	
TMA-E	3.7×4.8[001]		
Edingtonite	3.5×3.9[110]		
Epistilbite	3.7×4.4[001]	3.2×5.3[100]	
Erionite	3.6×5.2[001]		
Faujasite			7.4<111>
Ferrierite	3.4×4.8[010]	4.3×5.5[001]	
Gismondine	3.1×4.4[100]		
	2.8×4.9[010]		
Gmelinite	3.6×3.9[001]		7.0[001]
Heulandite	4.0×5.5[100]	4.4×7.2[001]	
	4.1×4.7[001]		
ZK-5	3.9<100>		
Laumontite		4.0×5.6[100]	
Levyne	3.3×5.3[001]		
Type A	4.1<100>		
Type L			7.1[001]
Mazzite			7.4[001]
ZSM-11		5.1×5.5[100]	
Merlinoite	3.1×3.5[100]		
	3.5×3.5[010]		
	3.4×5.1[001]		
	3.3×3.3[001]		
ZSM-5		5.4×5.6[010]	
		5.1×5.5[100]	
Mordenite	2.9×5.7[010]		6.7×7.0[001]
Natrolite	2.6×3.9<101>		
Offretite	3.6×5.2[001]		6.4[001]
Paulingite	3.9<100>		
Phillipsite	4.2×4.4[100]		
	2.8×4.8[010]		
	3.3[001]		
Rho	3.9×5.1<100>		
Stilbite	2.7×5.7[101]	4.1×6.2[100]	
Thomsonite	2.6×3.9[101]		
	2.6×3.9[010]		
Yugawaralite	3.1×3.5[100]		
	3.2×3.3[001]		

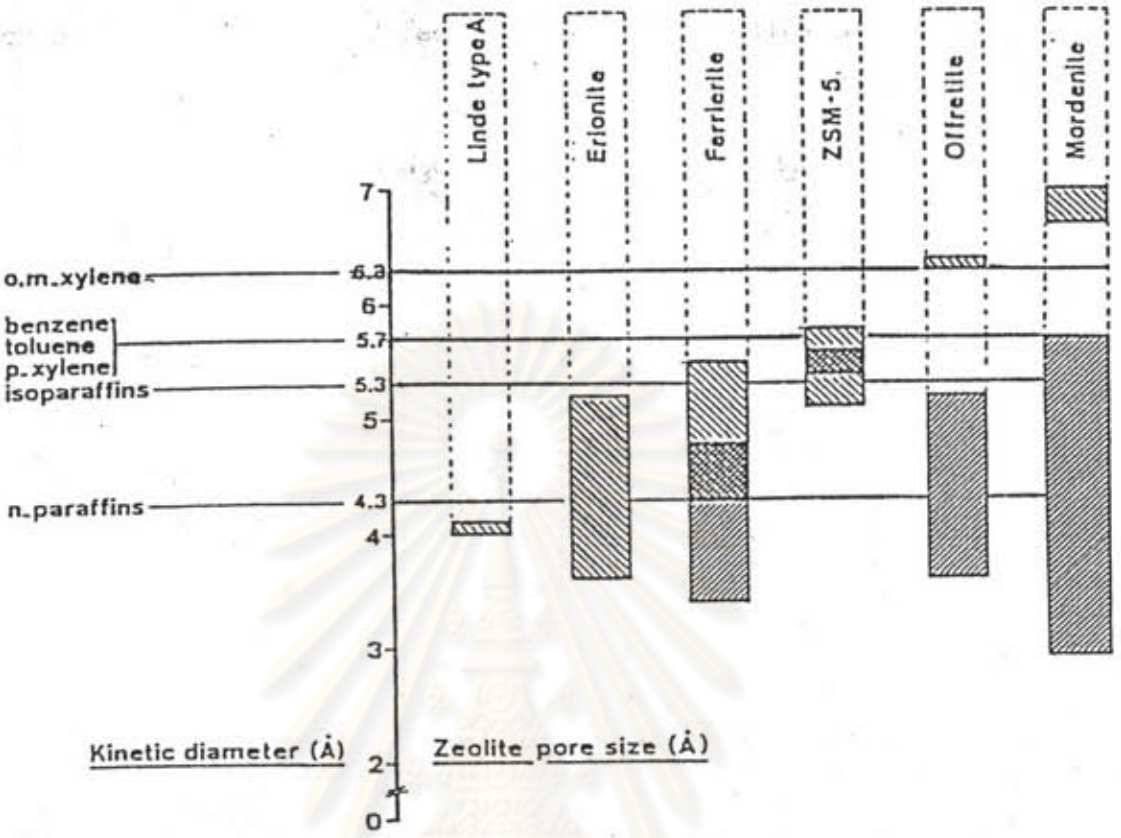

Figure 3.12 Correlation between pore size(s) of various zeolites and kinetic diameter of some molecules [64].

Voltz and Wise [66] has proposed the modified scheme, Scheme B, to contain a direct path to olefins from methanol:

$$2CH_3OH \rightleftharpoons CH_3OCH_3 + H_2O$$

$$\searrow \quad \swarrow$$

olefins

Scheme B

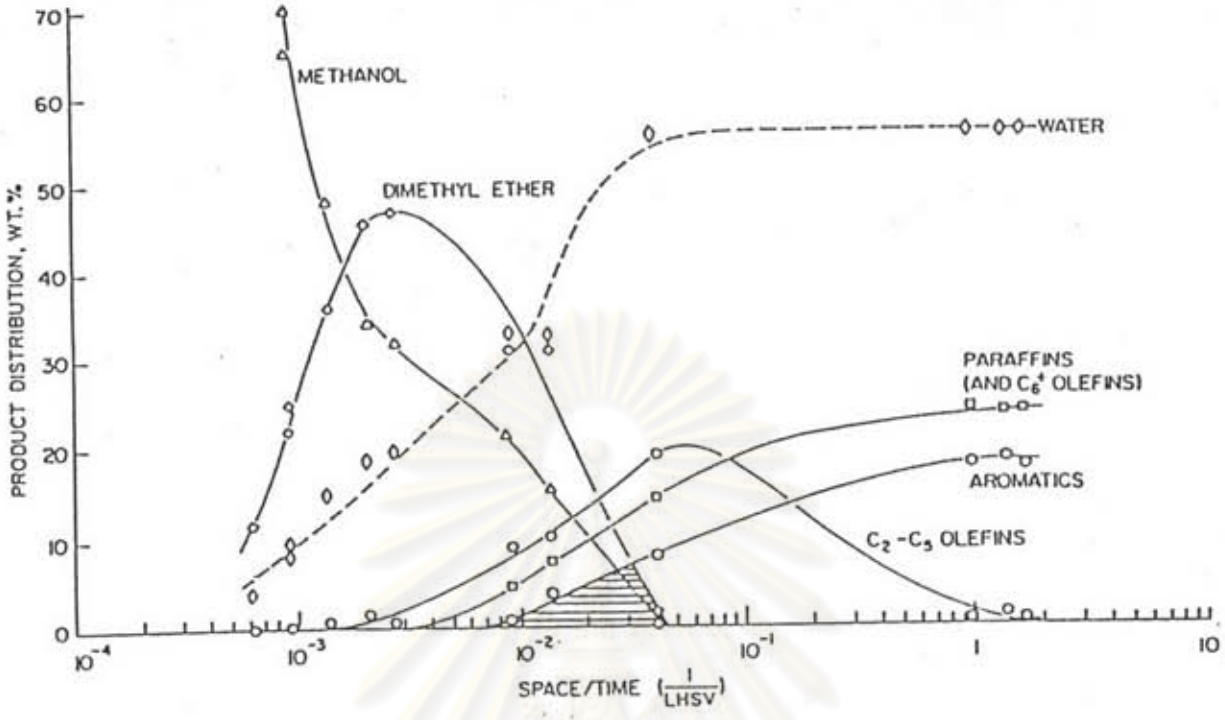

Figure 3.13 Reaction path for methanol conversion to hydrocarbon over H-ZSM-5 (371°C) [5].

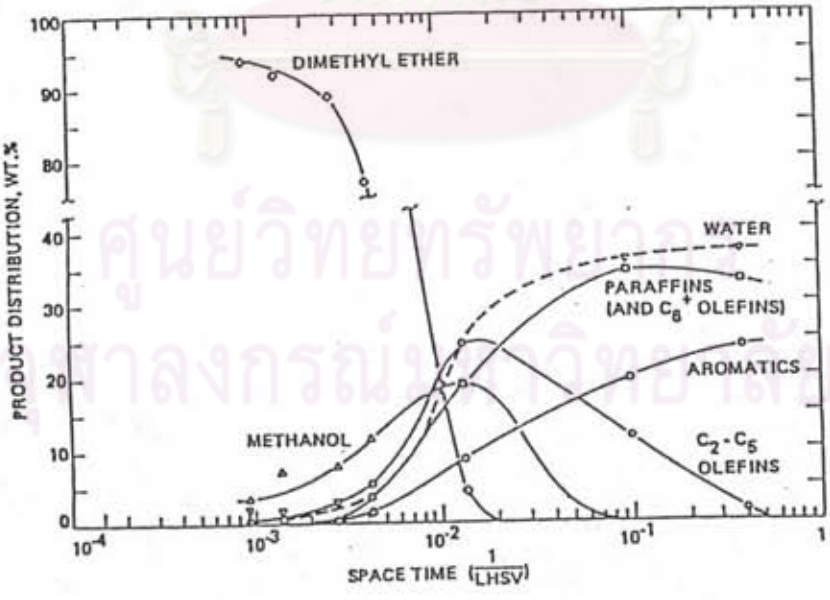

Figure 3.14 Reaction path for dimethyl ether conversion to hydrocarbons over H-ZSM-5 (371°C) [5].

The reaction path formation may be viewed essentially as composed of three key steps - ether formation, initial C-C bond formation, and aromatization with H-transfer. The final stages, comprising olefin condensation, cyclization and H-transfer over acidic catalysts, have been well studied and proceed via classical carbenium mechanisms [68-70].

The mechanism of polymethylbenzenes formation will, however, be discussed since these compounds are peculiar to the methanol transformation reaction.

3.5.1 Ether formation

The mechanism of ether formation from alcohols over oxide catalysts, particularly Al_2O_3, has been extensively investigated. The bulk of work has concentrated on alcohols having α-hydrogens. Several comprehensive surveys have been published [71-73].

In contrast, the literature on methanol dehydration is relatively sparse. Methanol etherification is similar in many respects to that of the higher alcohols; however, since methanol lacks a parent olefin, sufficient differences may be found as to warrant its discussion here.

The dehydration of methanol on alumina and amorphous silica-alumina monitors the effect of a series of nitrogenous poisons (various amines and N-heterocycles) or dimethyl ether formation. Silica-alumina is irreversibly poisoned, while alumina is reversibly poisoned. This is taken as evidence that the reaction

over alumina involved surface methoxy groups:

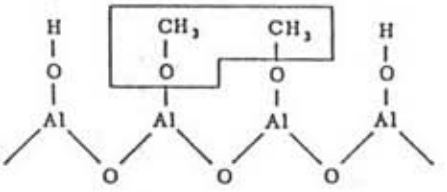

This interpretation is based on the assumption that bases such as diethaylamine dissociatively but reversibly chemisorb on alumina.

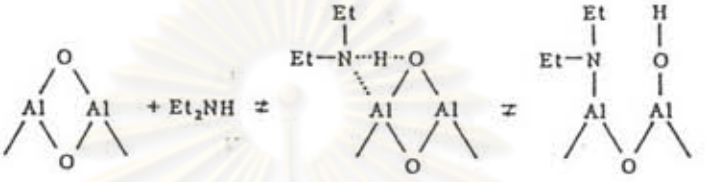

Because of the greater nucleophilicity of N vs O, the nitrogenous base competes with methanol for the surface oxygen, thereby inhibiting methoxylation. On the other hand, the reaction over silica-alumina involves Bronsted sites, which are strongly poisoned by nitrogen base, forming stable quaternary ions. According to these investigators ether formation over silica-alumina may be represented by the following scheme:

$$CH_3OH + H^+ \longrightarrow CH_3OH_2^+$$

$$CH_3OH_2^+ + CH_3OH \longrightarrow (CH_3)_2O + H_2O + H^+$$

The kinetics of methanol dehydration over silica-alumina at 160-200 ^oC and the rate expression can derive as follow:

$$v = ka\sqrt{P_a}/(1+a\sqrt{P_a})$$

where P_a is the alcohol partial pressure. It was concluded that the rate-limiting step cannot be the interaction of two surface

alcoholate groups, which would lead to a rate equation of the form

$$r = k\theta^2 = kaP/(1+aP)^2$$

At low pressures the reaction order would be unity, which is not in agreement with the observed half-order. Figueras et al. proposed two modes of chemisorption, both of which assumed the concerted action of acidic and basic centers. Nucleophilic attack on carbon by the basic site would generate CH_3^+, which then interacts with an acid-generated surface methoxy group to give ether. The observed half-order was rationalized on the ground that one of the species, CH_3O or CH_3, must be reversibly adsorbed. Primary carbonium ions are much less stable than alkoxide structures, and therefore equilibrium with the undissociated species would be readily established:

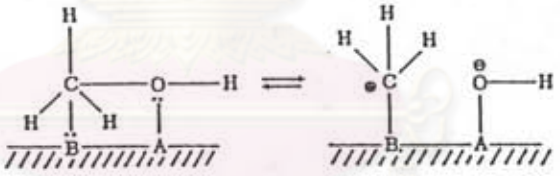

The thermal decomposition of methanol adsorbed on alumina was investigated by using deuterium labeling. Desorption of methanol started at 77°C. At T > 77°C, significant concentrations of CH_2O, H_2O, and CH_3OCH_3 were observed, and above 427°C, CO was predominant while CH_4 was significant. Coadsorption of CD_3OD and CH_3OH was carried out. Under desorption at T < 237°C, the ether contained only CH_3OCH_3, CH_3OCD_3, and CD_3OCD_3, while at higher temperatures deuterium distribution became random. Thermal decomposition of CH_3OH_{ad} in the presence of gaseous CD_3OCD_3 gave only CH_3OCH_3,

indicating that ether is formed by a bimolecular reaction between adjacent surface methoxides.

Schmitz [74] studied the dehydration of methanol over silica-alumina at 289-418 ^{o}C and found that the reaction becomes first-order in methanol at the higher temperatures. Interestingly, Schmitz observed an induction period, possibly the result of the initial formation of surface carboxylate groups, which, though not ether intermediates, could nevertheless influence the initial rate of dehydration by occupying active sites. Another explanation might involve competitive sorption of product water prior to establishment of steady-state with respect to surface hydroxyl concentration.

Detrekoy and Kallo [75] investigated the dehydration of methanol over clinoptilolite by infrared spectroscopy. Methanol (6 torr) was adsorbed on H-clinoptilolite at various temperatures. At 25^{o}C the 3620 cm^{-1} band (acidic OH on clinoptilolite) disappears and two bands at 2950 and 2840 cm^{-1} (CH stretching) appear. Upon evacuation, the CH bands decreased significantly; however. the OH band did not reappear. This indicated that only weakly adsorbed methanol is removed. Absorption at 160^{o}C followed by evacuation caused only a partial disappearance of the 3620 cm^{-1} band and a lower intensity of the 2950 and 2840 cm^{-1} bands. At 400^{o}C, methanol can be completely removed and the CH bands are shifted to 2860 and 2960 cm^{-1}, indicating the presence of surface methoxyls.

Detrekoy and Kallo found that methanol dehydration also occurs on dehydroxylated (at T > 400^{o}C) clinoptilolite. They attribute this to the formation of Bronsted sites from Lewis sites by hydration during reaction with methanol. The following mechanism

was proposed:

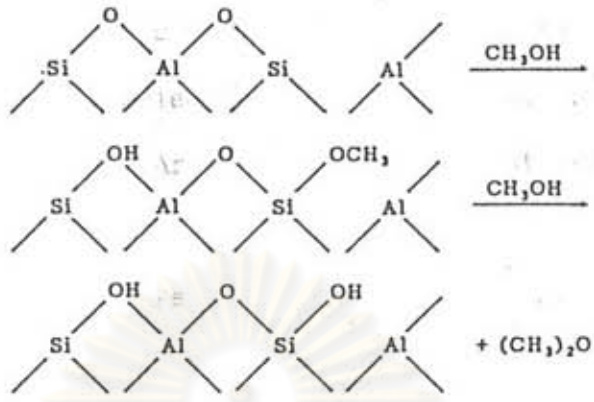

Further reaction would be catalyzed by the acidic OH groups thus generated.

In a study of methanol reaction on synthetic germanic near-faujasite using ^{13}C-NMR, Derouane et al. [76] observed partial methoxylation of the surface at 300°C, with ether formation. Surface methoxyls could be hydrolyzed with water back to methanol at 25°C. Additional small amounts of dimethyl ether and surface formate were also found after hydrolysis.

In summary, the weight of evidence favors the intermediacy of surface alkoxyls in ether formation from alcohols. Beranek and Kraus [77] conclude that the mechanism involves essentially a nucleophilic substitution whereby the surface alkoxide is attacked by another molecule, either from the gas phase or from a weakly adsorbed state. Arguments in support of this mechanism were summarized as follows:

1. "Similar products are obtained by the decomposition of metal alkoxides containing no β-hydrogens and by the reaction of corresponding alcohols on alumina at lower temperatures".

2. "Acetic acid and pyridine are poisons for the formation of ethers".
3. "The different degrees of water inhibition on the ether and olefin formation from ethanol on alumina, and the agreement of ether/ethylene selectivity ratios found experimentally with those calculated by the Monte Carlo simulation of the hydrated surface of alumina".
4. "Correlation between the rate of ether formation from ethanol and the surface concentration of ethoxide species determined by IR spectroscopy".
5. "The positive value of the Taft reaction parameter for the formation of ether in contrast to negative values for the olefin formation on the same catalyst".

The second part of Statement 5 applies only to C_2^+ alcohols.

3.5.2 Hydrocarbon Formation

The mechanism of initial C-C bond formation from methanol is an unresolved question at present. Hypothetical mechanisms abound in the literature, and run the gamut from carbene to free radical schemes. As of this writing, however, little supporting experimental evidence has appeared. It seems appropriate, nevertheless, to survey and discuss the diverse entries in this "mechanism sweepstakes."

3.5.2.1 Via Surface Alkoxyls

Among contemporary investigators, the first to consider this question were Topchieva and collaborators in connection with a study of the adsorption of methanol vapor on SiO_2, SiO_2-Al_2O_3, and Al_2O_3 surfaces. It was found that a portion of the methanol was irreversibly adsorbed on SiO_2-Al_2O_3 and Al_2O_3, which upon heating and pumping to 400°C evolves C_2H_4, C_2H_6, CO, and CO_2. The formation of surface methoxy groups was regarded as the primary step. Hydrocarbon formation was considered to occur by condensation of methoxy groups, accompanied by dehydration and H-transfer. The mechanistic details of this condensation were not specified. Subsequently, Heiba and Landis [78] showed that the thermolysis products of aluminum alkoxides are virtually identical to the products of alumina-catalyzed decomposition of alcohols or ethers, as shown in Table 3.3. It is seen that the main products are CH_4, H_2, CO, $(CH_3)_2O$, and smaller amounts of C_2H_4 and C_3H_6. Based on the observation that $Al(OCH_2\Phi)_3$ decomposed more readily than $Al(OCH_3)_3$, it was concluded that cleavage of the C-O bond is a heterolytic process, with the flow of electrons in the direction of Al, leaving a positively charged carbon moiety as the reactive intermediate. A negative activation entropy was observed, suggesting a cyclic transition state. A free radical mechanism was rejected on the basis of negligible reactivity over nonacidic solids, e.g., quartz, at temperatures up to 450°C.

In a later study the thermal decomposition of methoxides of Na, Mg, and Al and the compound $Na[Al(OMe)_4]$ was

Table 3.3 Decomposition of Methyl Derivatives [78].

Product	$Al(OCH_3)_3$ at 385°C (mol%)	CH_3OH over Al_2O_3 at 450°C, 0.5 LHSV	$(CH_3)_2O$ over Al_2O_3 at 450°C, 0.5 LHSV
CH_4	22.5	Major	Major
H_2	35.2	Major	Major
CO	31.1	Major	Major
C_2H_4	1.3	Minor	Minor
C_3H_6	2.5	Minor	Minor
$(CH_3)_2O$	7.1	Major	Major
Other	0.3	Minor	Minor

reported by Pfeifer and Flora [79]. Ethene was the only hydrocarbon product observed.

3.5.2.2 Carbenes and Carbenoids

Venuto and Landis proposed an α-elimi-nation mechanism to account for olefins formed during methanol dehydration to dimethyl ether over NaX at 260°C, as reported by Mattox [80], and from methanol reaction over ReX and ZnX at 330-390 °C, as observed by Schwartz and Ciric [81]. According to this view, methanol adsorbed on the zeolite surface loses water to form a divalent carbenoid species, which then polymerize to form olefins:

$$H\text{-}CH_2\text{-}OH \longrightarrow H_2O + :CH_2$$

$$n{:}CH_2 \longrightarrow (CH_2)_n, \quad n = 2, 3, 4, 5$$

Swabb and Gates studied the dehydration of methanol over H-

mordenite at 155-240 °C. Traces of olefin were detected at 240°C. It was speculated that the olefins were formed by an α-elimination mechanism. where bond scission is facilitated by cooperative action of acidic and basic sites in the zeolite lattice:

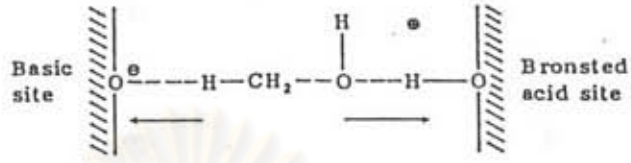

Salvador and Kladnig [82] investigated the surface reactions of methanol on HY and NaY at 20-350 °C using IR, GLC, adsorption isotherm, and TGA techniques. At room temperature, physical adsorption occurs on both zeolites. With HY, methoxylation of surface hydroxyl groups begins at 20°C, reaching a maximum at 130°C. At 120°C, dimethyl ether formation begins and reaches a maximum at 210°C, and around 250°C secondary cracking reactions occur forming predominantly butane and propene. This was accompanied by darkening of the catalyst due to coking which was enhanced with a further temperature increase. Salvador and Kladnig favored an α-elimination mechanism to explain olefin formation. They differed with the acid-base mechanism of Swabb and Gates, proposing that the generation of carbenoid species occurs by decomposition of the methoxylated surface:

$$\equiv SiOCH_3 \longrightarrow \equiv SiOH + :CH_2$$

Condensation of the carbene would give olefin. Alkanes were assumed to arise via H-transfer reactions.

An α-elimination mechanism involving a

carbenoid intermediate was also proposed by Chang and Silvestri for methanol reaction over ZSM-5. However, it was considered unlikely the olefins were formed by polymerization of the diradical intermediate. On view of the high reactivity of carbenes, the probability of such an event would be low, as demonstrated in studies on ketene photolysis. By the same taken, the presence of free carbenes would be unlikely. Rather, a concerted reaction between methylene donor and acceptor was proposed involving simultaneois α-elimination and sp^3 insertion into methanol or dimethyl ether as the primary step.

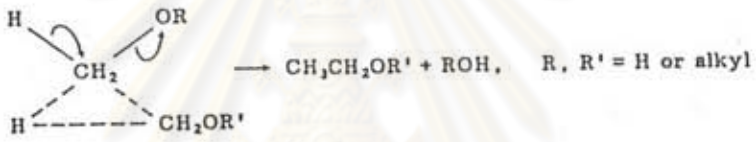

An ionic mechanism involving methyl cations was rejected since these species would be expected to form methane readily via hydride abstraction from methanol, dimethyl ether, or hydrocarbons. The reaction

$$CH_3^+ + CH_3OH \longrightarrow C^+H_2OH + CH_4$$

is extremely rapid in the gas phase. However, methane normally accounts for $\leq$ 1% of the hydrocarbons formed over ZSM-5. Note also that C^+H_2OH could deprotonate to formaldehyde which is not observed over ZSM-5.

The presence of small amounts of methyl ethyl ether in the products of methanol conversion over ZSM-5 was reported by Chang and Silvestri. Cormerais et al. found MeOEt among

the products of dimethyl ether decomposition over silica-alumina at 423 K. This compound could either be a key reaction intermediate or simply a secondary product of the methanol-to-ethene reaction. From kinetic evidence, Cormerais et al. deduced that this compound was not formed via reaction of Me_2O with ethene. It was determined that in the presence of excess ethene, amounting to 30X that of the products from Me_2O, the rate of MeOEt formation from Me_2O was increased by only a factor of 5. More significantly, the formation of propene from MeOEt was more than 10 times faster than from Me_2O. In view of the observed unreactivity of ethene, it was concluded that propene is formed by two successive CH_2 insertions into Me_2O, leading to MeOPr, which cleaves to propene. Another set of experiments gave analogous results for C_4 hydrocarbons. Cormerais et al. [83,84] proposed a chain growth "rake mechanism," Figure 3.15, to explain their results. In this scheme, chain growth occurs by carbene insertion into surface alkoxy species, which are transformed into olefins via carbenium ions.

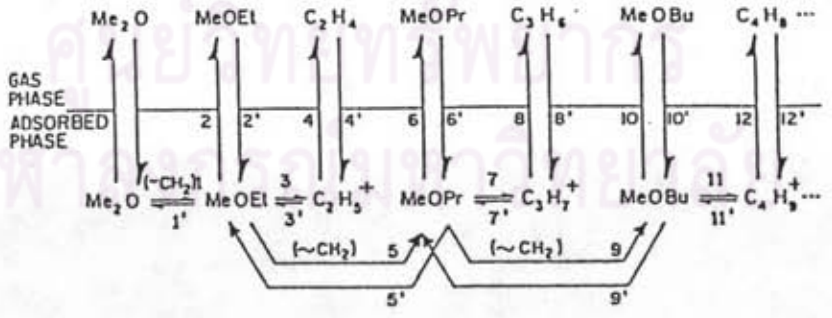

Figure 3.15 "Rake" mechanism for dimethyl ether conversion to hydrocarbons [83].

Chang and Chu [85] reported that when methanol is reacted over ZSM-5 in the presence of propane, the usual high iso-to-normal ratio of product butanes is significantly lowered. This is shown in Table 3.4 where the butane i/n is seen to be 3.8 for the control experiment and 1.1 when propane is added. The thermodynamic equilibrium i/n is 0.75 at the reaction conditions. However, under the same conditions propane and isobutane were virtually inert in the absence of methanol. In the presence of $^{13}CH_3OH$ (90% ^{13}C, 10% ^{12}C), it was found that the selectivity to singly-labeled butanes was 30-45 times higher than that expected from random distribution. It was concluded that propane methylation had occurred. Further, the butane i/n increased with increasing ^{13}C

Table 3.4 Effect of Propane on Methanol Conversion over H-ZSM-5[a][85] (370°C, 1 atm, 0.4 h^{-1} LHSV (CH_3OH))

Hydrocarbon product (wt%)[b]	CH_3OH/He	CH_3OH/C_3H_8
CH_4	0.86	0.90
C_2^0	0.93	0.90
C_2^{2-}	2.35	2.36
(C_3^0)	-[c]	-[d]
C_3^{2-}	3.63	4.53
i-C_4^0	35.17	23.14
n-C_4^0	9.20	20.24
C_4^{2-}	1.88	2.34
C_5^+ aliphatic	21.32	20.98
Aromatics	24.66	24.62
	100.00	100.00
i/n C_4^0	3.8	1.1

[a] Three moles CH_3OH/1 mole diluent.
[b] Normalized on a propane-free basis.
[c] Actual C_3^0 = 25.36% of hydrocarbon.
[d] Net conversion of C_3^0 ~5%.

substitution. The i/n of the $^{13}C_4H_8$ is 2.8, and reflects the fact that they arise primarily from self-reaction of $^{13}CH_3OH$. The singly-substituted butanes, mostly the product of methylation, have i/n 1, close to the equilibrium value. From these considerations it was deduced that the reactive C_1 intermediate is carbene-like, and the mode of attack is insertion into an sp^3 C-H bonds of the substrate being subject to attack with equal probability:

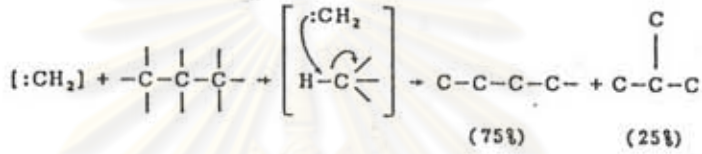

although for a homogeneous gas-phase reaction there is some evidence of discrimination in favor of secondary over primary C-H bonds. In the CH_3OH/C_3H_8 reaction, carbene insertion will lead statistically to higher concentrations of n-butane relative to i-butane. Attack by a cationic species such as CH_3^+ or methyloxonium ion according to an Olah-type mechanism (vide infra), on the other hand, will yield high i/n butane ratios due to stability of tertiary carbenium ions in the transition state. In the methylation of propane with the CH_3F-SbF_5 complex in SO_2ClF, for example, CH_4 is formed via H-transfer, and i-butane is the major alkylation product. The following pathway has been proposed to account for i-butane formation:

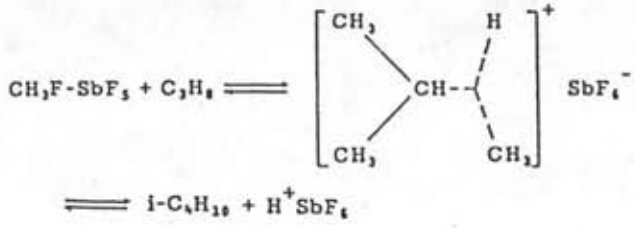

The alternative to sp^3 C-H insertion, namely C_1 addition to the double bond of propene generated from propane via dehydrogenation, also received consideration. Although propane itself is largely unreactive, it was believed possible that the unfavorable dehydrogenation equilibrium could be displaced by a "drain-off" reaction involving addition of a highly reactive species across the double bond of propene. Carbene addition would yield, classically, methylcyclopropane. However, subsequent protonation and rearrangement gives preferentially the tertiary butyl cation, which will either yield 2-methylpropene via loss of a proton, or i-butane via H-transfer. If the attacking species were cationic, branched products would similarly result:

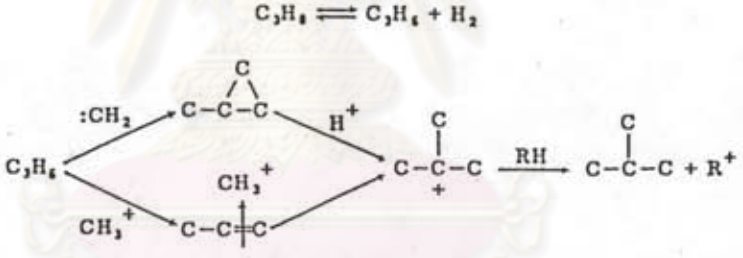

Another pathway involving propylium ion as an electrophile can also be written:

$$C_3H_6 \overset{H^+}{\rightleftharpoons} C_3H_7^+ \overset{:CH_2}{\longrightarrow} iC_4H_9^+$$

but leads to the same conclusion. This alternative was therefore rejected as an explanation of the observed results. However, in the case of reaction of methanol alone, these mechanisms, with propene

as an intermediate, can be invoked to explain the characteristic high i/n butane selectivity.

In another attempt at "trapping" the reactive C_1 intermediate. Chang and Lang reacted methanol over H-ZSM-5 in the presence of acetonitrile. It was reasoned that a carbene would insert mainly into the C-H bonds and to a lesser extent, add to the C N group. A cationic intermediate, on the other hand, would attack the C N electron system exclusively, forming a nitrilium ion:

$$CH_3^+ + CH_3C\text{-}N \longrightarrow CH_3C^+ N\text{-}CH_3$$

Upon hydrolysis, N-substituted acetamides would result. This is a Ritter-type sequence. Carbene addition to the C-N group would result in a highly reactive azirine intermediate, which would yield the same nitrilium ion in the presence of acidic catalysts. Thus the sole presence in the final product of N-substituted acetamides would be evidence of a cationic intermediacy (although the alternative of acetamide formation via reaction of amines with acetic acid from acetonitrile hydrolysis cannot be ruled out). On the other hand, the presence of higher nitriles, with or without the acetamides, must be taken as a strong indication of carbene involvement. It was also found that acetonitrile, itself stable over the temperature range of interest, served to moderate the reaction by competing strongly for the acid sites.

At 454°C an equimolar mixture of methanol and acetonitrile gave mostly acetic acid and methylamines (36%

methanol conversion). This is the result of acetonitrile hydrolysis and methanol amination. At 496°C (79% methanol conversion), hydrocarbons, CH_3CH_2CN, and N-substituted acetamides were in evidence, as well as CH_3COOH + $C_{H3}COOCH_3$, and methylamines.Upon raising the temperature to 538°C, the reactor effluent contained 16.3% hydrocarbons and 7.0% O- and N-compounds (exclusive of unreacted acetonitrile). These O- and N-compounds consisted of 12.8% CH_3COOH + CH_3COOCH_3, 46.6% CH_3CH_2CN, 37.2% N-methyl-ω-aminonitriles, and 3.4% higher esters, pyrroles, etc.

The CH_3CH_2CN is taken as evidence of carbene insertion, while the N-methyl-ω-aminonitriles may result from an analogous nitrenium insertion where the nitrenium ion is generated from a methylamine precursor:

$$R_1R_2R_3N \longrightarrow R_1R_2N^+: + :R_3$$

$$R_1R_2N^+: + CH_3CN \longrightarrow R_1R_2N^+{:}CH_2CN \longrightarrow R_1R_2NCH_2CH$$

(H above the second N; $-H^+$ above the arrow)

The reaction of methanol in the presence of zinc iodide at 200°C was reported by Kim et al. to yield highly branched hydrocarbons. Particularly high selectivity to triptane was observed. They postulated that the intermediate is a carbene complexed with the salt, similar to the Simmons-Smith reagent (CH_2I_2 + Zn(Cu)), which reacts with alkenes to form cyclopropane derivatives via carbene addition to the double bond.

3.5.2.3 Oxonium Ions and Yields

In their mechanism Chang and Silvestri left open the question of stabilization of the intermediate carbene in the transition state. A plausible resolution of this question may be found in the mechanism of van den Berg et al. [86]. In their view, dimethyl ether from methanol dehydration reacts with a Bronsted acid site to form a dimethyloxonium ion I, which reacts with another molecule of dimethyl ether to form, via II, and after elimination of methanol, a trimethyloxonium ion III:

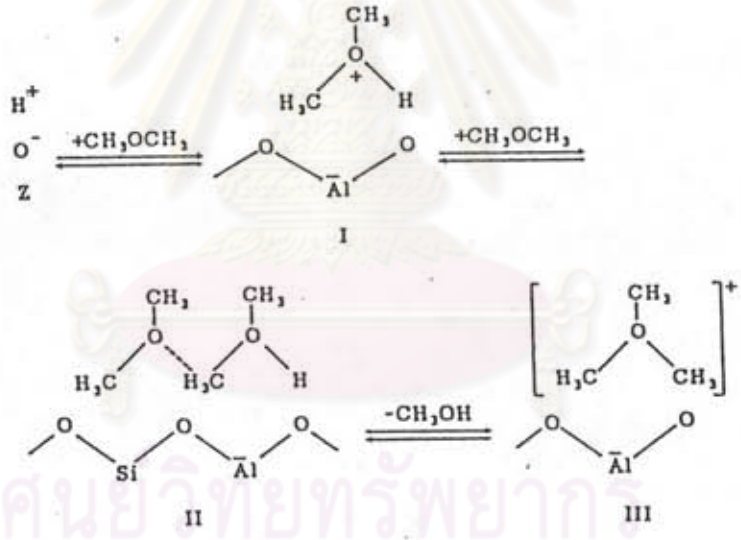

the critical step in their proposal is a Stevens-type intramolecular rearrangement of the trimethyloxonium ion III to a methyl ethyloxonium ion V:

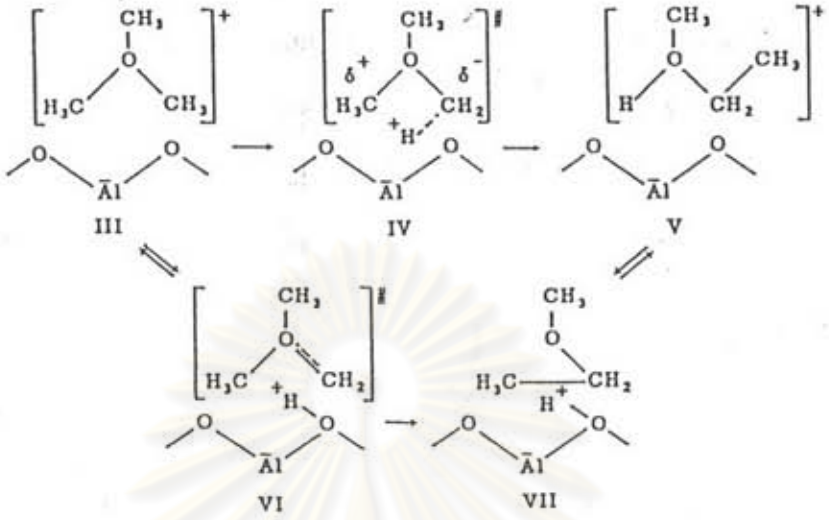

Structure VI, which is equivalent to the oxonium ylid $(CH_3)_2O^+CH_2^-$, is seen to contain the stabilized C_1 carbenoid species. Cis-insertion of the carbenoid into the adjacent C-O leads to C-C bond formation. The formation of ylid depends on the assumption that the conjugate basic sites in ZSM-5 are sufficiently strong to induce polarization of a C-H bond on a methyl group. As indicated previously, the ab initio field calculations of Beran and Jiru [87] lend support to this assumption.

An alternate cationic mechanism involving carboxonium ions was considered by van den Berg [88]. In this variation the carboxonium ion is generated by hydride abstraction. Van den Berg presented the following scheme comparing the steps in the alkoxonium Route (A) and the carboxonium Route (B).

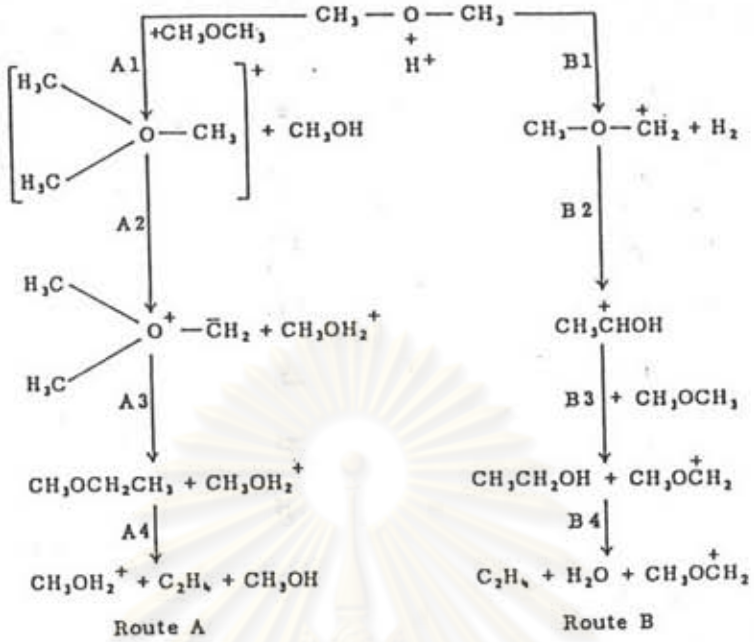

A major difference is found between Steps A2 and B2. However, ab initio calculations indicate that although the 1-hydroxyethyl cation is more stable than the methoxymethyl cation, the energy barrier separating the two is on the order of 260 kJ/mole, assuming that the rearrangement proceeds through the O-protonated oxirane:

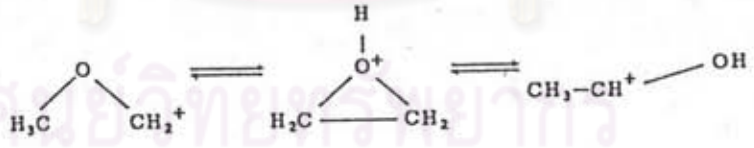

this is comparable to the expected energy barrier of Step A2. Step A3 is highly exothermic and, in view of the behavior of the N-analogue, is expected to have a low activation energy. Figure 3.16 is an energy diagram comparing Routes A and B. It was concluded that Route A, involving the trimethyloxonium ion, is favored.

According to van der Berg, kinetics of dimethyl ether reaction over H-ZSM-5 is zero-order at 227-300 ^{o}C. Chang

and Lang found the reaction order of methanol decomposition over H-ZSM-5 at 371°C to be zero-order up to about 60% conversion, and increasing in order at higher conversions, suggestive of Langmuir-Hinshelwood behavior. This is consistent with van den Berg's proposal that the formation of adsorbed alkoxyoxonium species is favored, with the C-C bond of formation as the most demanding step. However, van den Berg observed an anomalous temperature effect, illustrated in the Arrhenius plot of Figure 3.17. To explain this phenomenon it was proposed that at 227-260 °C, C-C bond formation proceeds via the intramolecular rearrangement of trimethyloxonium

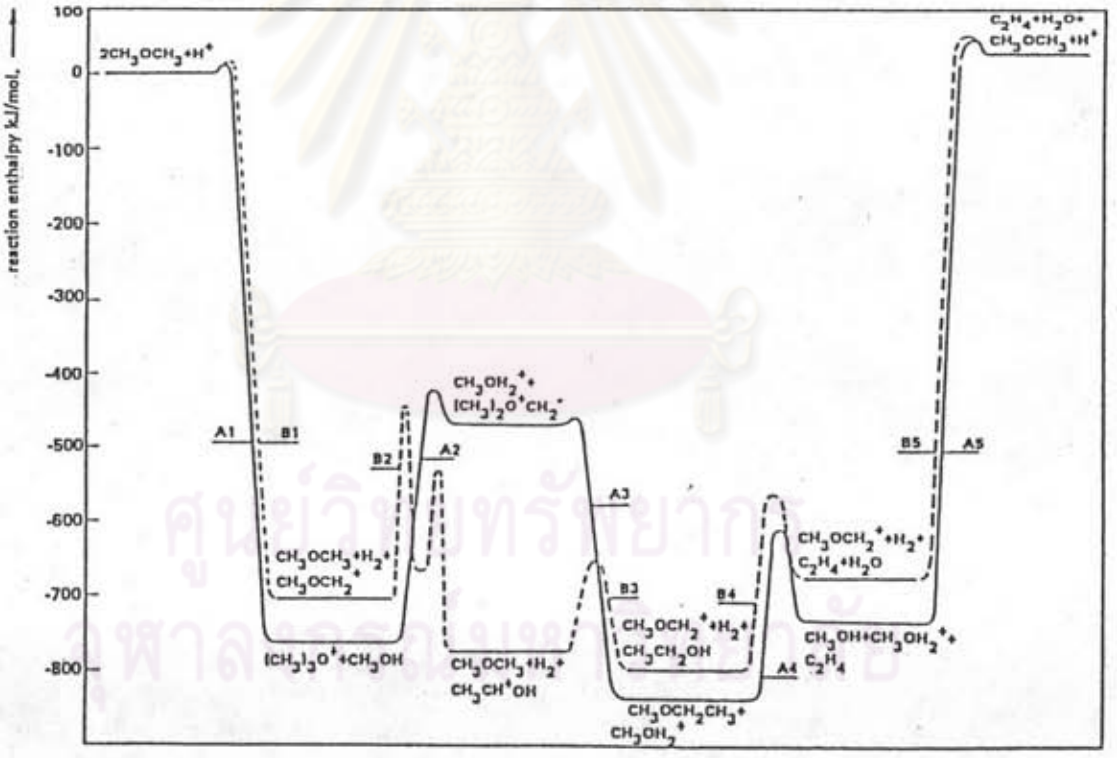

Figure 3.16 Energy diagram for Routes A and B [88].

ions while at higher temperatures a concerted reaction between dimethyl ether and alkyl cations, with the oxonium ion as the tran-

sition state, becomes significant.

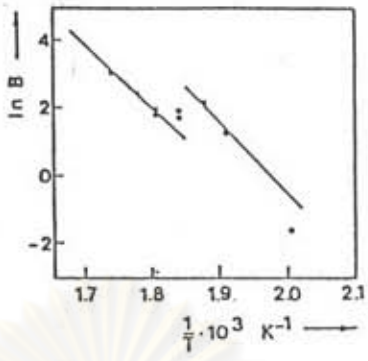

Figure 3.17 Arrhenius plot of the dimethyl ether conversion on zeolite H-ZSM-5 [88]. P_X = 50.7 kPa; WHSV = 0.72 h^{-1}.

It should be noted that ylid mechanisms have been earlier proposed to explain C-C bond formation from organic N and S compounds in the presence of zeolites. One such example is the formation of stilbene from benzyl mercaptan over Na13X reported by Venuto and Landis [89]. Although these workers preferred an α-elimination mechanism for this reaction, they recognized that a sulfonium ylid mechanism is also possible. Wu wt al. [90] studied the thermal decomposition of methylammonium cation exchanged Y-type faujasites. At 275-450 °C, ethene was observed among the products of decomposition. To account for this result, a mechanism involving a Stevens rearrangement followed by Hofmann elimination was proposed

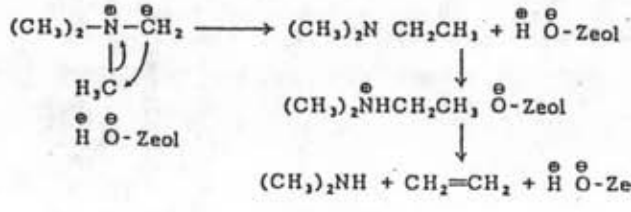

In another example (not involving zeolites) reported by Lepley and Giumanini [91], the thermolysis of N,N-

dimethylpyrrolidinium bromide gives N-ethylpyrrolidine by carbene insertion:

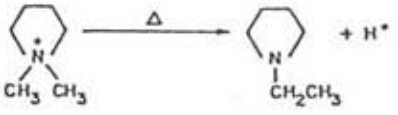

The Stevens rearrangement of oxonium compounds has not been reported up to this time. However, the insertion of CH_2, generated by ketene photolysis, into C-H bonds of alkyl ethers is believed to occur via an ylid intermediate. No insertion into alkyl ether is observed when the methylene is generated by mercury photosensitization, indicating that singlet methylene is involved in the attack. Methylene generated from diazomethane by cuprous halide-catalyzed decomposition was similarly ineffectual. However, when the substrate contains an electron-withdrawing group, reaction with diazomethane occures, as in the following reaction reported by Meerwein et al. [92]:

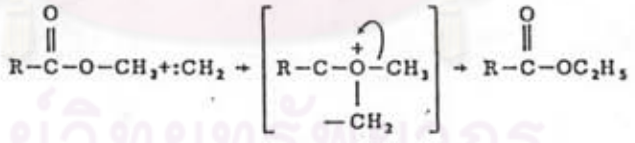

Methanol conversion over phosphorus-modified ZSM-5 was studied by Kaeding and Butter, who proposed the following mechanism based also on oxonium intermediates:

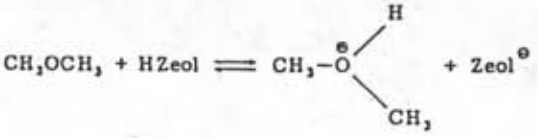

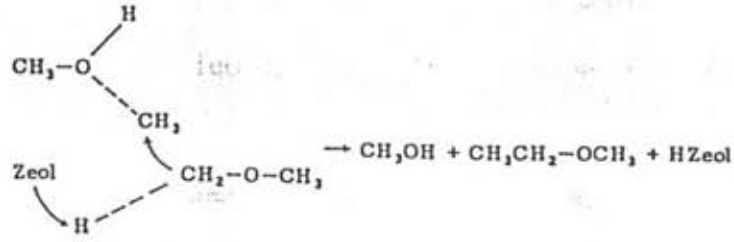

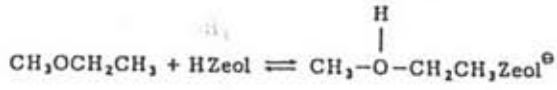

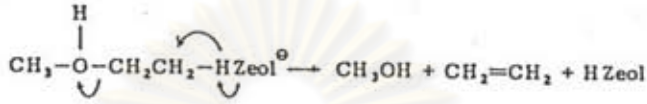

The key step in this mechanism is the labilization of a C-H bond, assisted by anionic sites in the zeolite. The resultant nucleophilic species then attacks the "incipient methyl carbonium ion" from protonated methyl ether (or methanol).

3.5.2.4 Carbenium Ions and Superacid Chemistry

Mechanisms based on electrophilic attack bymethyl cations at saturated carbon are favored by some workers. Such reactions were first observed insuperacid media by Olah and co-workers and are exemplified by the remarkable reaction of methane:

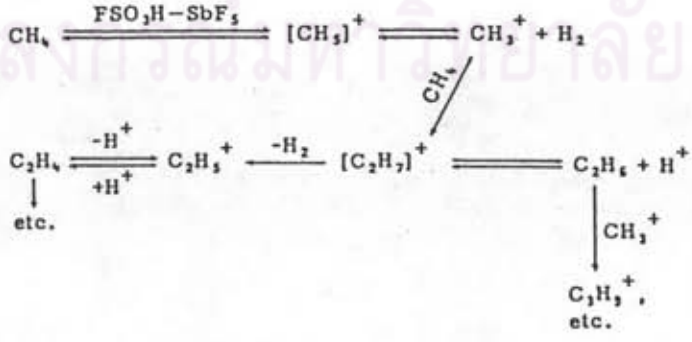

The transition state is believed to be a pentacoordinate carbonium ion, typified by the CH_5^+ methanonium ion shown above, and in the following substitution reaction:

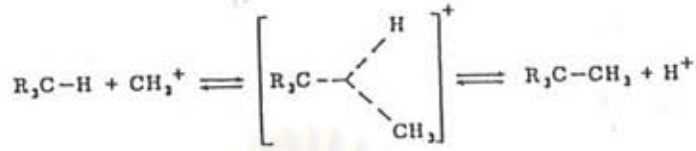

Pearson [93] proposed this as a possible mechanism of C-C bond formation in methanol decomposition by phosphorus pentoxide.

Based on their observation that methanol converts to hydrocarbons over heteropolyacids and Nafion-H (perfluorinated sulfonic acid resin), which are Bronsted acids, Ono and Mori [94] concluded that the mechanism involves methyl cations:

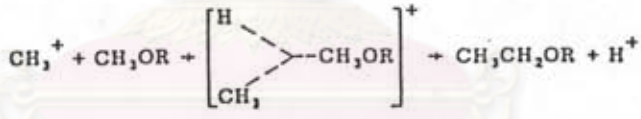

Generation of the methyl cation was considered to occur by polarization of surface methoxyl species:

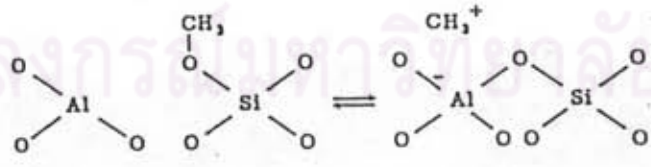

Autocatalysis involving condensation of methanol and olefins was cited as the reason why little methane is produced via hydride abstraction.

Ono et al. rejected the possibility of

carbene involvement. They found that HCl did not poison the methanol reaction over H-ZSM-5. They reasoned that since HCl poisons base-catalyzed reactions, basic sites do not participate in the reaction. They assert that these results "plead against the carbene mechanism, in which the abstraction of a proton from a methyl group by basic sites is essential."

The Olah superacid mechanism was also favored by Kagi [95], who proposed a series of oxonium intermediates, e.g.,

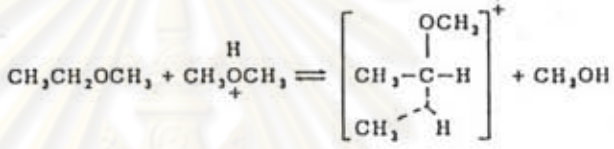

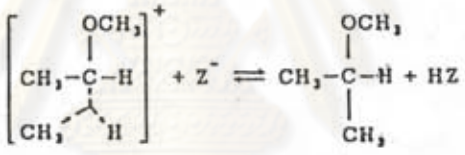

However, Chang considered the bulky transition states arising from such reactions improbable in ZSM-5 on account of limitations due to channel size.

It should be noted that neither CH_3^+ nor CH_5^+ have thus far been directly observed in superacid solutions. It has also been pointed out that SbF_5 and SO_3 are strong oxidizing species and could generate carbenium ions from alkanes by oxidation, although Olah points out that similar carbocation transformations are observed in systems such as HF-TaF_5 and HF-BF_3, which have high redox potentials, and therefore would not be potent oxidizing media.

Salem [96] has reported the conversion of methanol and dimethyl ether to hydrocarbons over TaF_5 and NbF_5.

At 300°C in an autoclave, a twofold excess of methanol was converted to a mixture of paraffins and aromatics. The NbF_5-catalyzed reaction gave more light hydrocarbons (>81% C_1-C_5) than the TaF_5 reaction (53% C_1-C_5). It was not clear whether the TaF_5 and NbF_5 were stable to hydrolysis under the reaction conditions or deactivated during the course of reaction.

The conversion of methanol over the alkylammonium zeolite Nu-1 was investigated by Spencer and Whittam [97]. They concluded that strong acidity is needed for the fast initial step and that cationic intermediates are involved. However, neither CH_3^+ nor oxonium ions were considered to be plausible.

3.5.2.5 Chain Mechanisms

Anderson et al., using deuterium labeling, found that in the methylation of benzene with methanol over H-ZSM-5 at 207°C, there is no exchange involving methyl hydrogens. From this it was inferred that in the methanol-to-hydrocarbon reaction, the initial step does not involve lability of the C-H bond prior to C-C bond formation, and that therefore the reactive intermediates are not carbene, carbenoid, or oxymethylene species. Instead, a active C_1 entity of the type $(CH_3)RO^+H$ (R = H or CH_3) was proposed, which participates in a chain propagation mechanism

$$\text{active } C_1 + \text{reactive } C_n \longrightarrow \text{reactive } C_{n+1}$$

where C_n is an olefin. This is a highly attractive scheme in that

it is consistent with the observed autocatalysis of the reaction. In such a scheme, moreover, the precise nature of the C_1 species becomes somewhat of a moot question. However, as has been noted, the temperature at which these D-labeling experiments were carried out was below the threshold for hydrocarbon formation from methanol in the presence of ZSM-5. Thus their bearing on the mechanistic question may be somewhat tenuous. The results of Matsushima and White [98] on deuterium exchange between CH_3OH and CD_3OD over alumina have already been mentioned. It will be recalled that these authors found little D-exchange below 237°C but complete scrambling at higher temperature ($T \geq 397^{o}C$).

3.5.2.6 Other Schemes

The conversion of methanol to C_1-C_5 hydrocarbons over natural mordenite was reported by Zatorski and Krzyzanowski, who proposed a free radical mechanism:

$$CH_3OH \longrightarrow CH_3 + OH$$
$$2CH_3 \longrightarrow C_2H_6$$
$$CH_3 + C_2H_6 \longrightarrow CH_4 + CH_3CH_2$$
$$CH_3 + CH_3CH_2 \longrightarrow C_3H_8$$
$$2CH_3CH_2 \longrightarrow C_4H_{10}$$
$$CH_3CH_2 \longrightarrow C_2H_4 + H$$

No supporting evidence was given. In this context it may be relevant that the Stevens rearrangement has been known to give rise to CIDNP

spectra, indicating some degree of radical involvement. A possible mechanism is dissociation into a radical pair within a solvent cage:

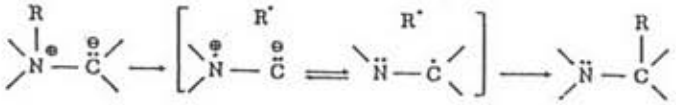

Lin et al. [99] studied methanol conversion over tungsten oxide on various supports including zeolite A, mordenite, and chabazite. A mechanism involving the formation of a "H_2C-O site" species as the rate-controlling step was proposed. "These species then migrate to sites where the external bonding between the sites and the oxygen is stronger than the internal bonding between C^+ and O^-. Divalent specie CH_2 is then formed and subsequently polymerized to produce the olefins." (It was not specified how charge conservation is to be preserved). The tungsten apparently has a dehydrogenation function.

Langner [100] proposed the following imaginative mechanism:

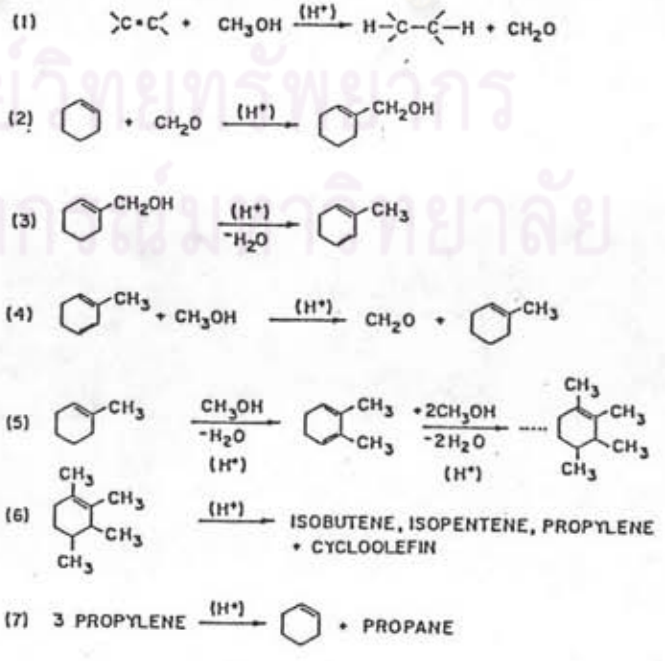

The critical steps are H-transfer from methanol to double bonds, producing formaldehyde (Steps 1, 4, 5); the Prins condensation of formaldehyde and cycloolefin (Steps 2, 5); dehydration of the hydroxymethyl substituent, followed by double-bond isomerization to the methyl derivative (Steps 3, 5); and generation of olefins from the polymethyl cyclic intermediate via the "paring reaction" (Step 6). The initial cycloolefin is generated according to Step 7.

According to Wu et al., the formation of methane, CO, and H_2 from zeolite surface methoxy species may proceed by a "methyl disproportionation" reaction which produces formaldehyde as an intermediate. An intermolecular hydride transfer is envisioned:

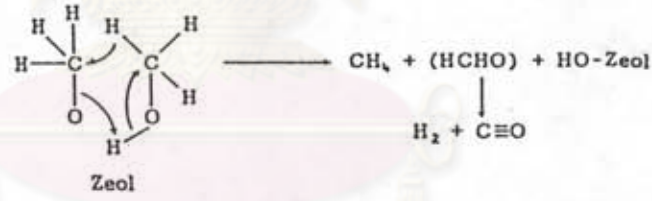

This reaction may also lead to coke formation:

$$HCHO \longrightarrow C + H_2O$$

Venuto and Landis considered methane to be formed from methanol via radical pathways.

Finally, hydride abstraction by the reactive C_1 species cannot be discounted as a source of at least some of the methane, usually present in minor amounts. As pointed out by Ono

et al., autocatalysis will minimize this reaction. However, hydride abstraction could be significant during the induction period of such autocatalysis and account for methane at low conversions.

3.6 Deactivation of Zeolites by Coke Formation

Carbonaceous residues are the inevitable by-products of most heterogeneously catalyzed organic conversions [101]. The term "coke" designates such deposits which often encompass mixture of hydrogen-difficient molecules which have hydrogen to carbon atomic ratio of 0.4-0.7. The formation of coke, affects both catalytic activity and selectivity (deactivation or aging), is most often acid catalyzed [102]. It is, therefore, a major concern when using solid acid catalysts, such as zeolites.

The model applicable to porous catalysts considers that coke deposits affect catalytic activity in two different ways, site coverage or poisoning(A) and pore blockage(B) [102]. Situation A is that of a poisoned site in an open pores whereas situation B corresponds to an inaccessible active site in a blocked pore. The kinetics of catalyst aging can then be expressed as a function of two probabilities; P(t) the probability for a site to be accessible at time t and S(t) the conditional probability that this particular site is not poisoned (covered) at the same time. P(t) depends on the structure of the zeolite pore network which controls the access to the active sites. S(t) is essentially related to the zeolite pore size which may impose constraints on the deposition of coke.

Recently, by quantitative approach, the deactivation of zeolites by coke formation is proposed to occur mainly through limitation or blockage of the access of the reactant to the active sites, not sites poisoning [103]. By their solubility in organic solvents, coke deposits can be categorized into soluble and insoluble coke. Since the major components of the soluble coke found were those polyaromatics of which boiling points were well below the reaction temperature. The soluble coke molecules were mecessarily located in the pore structures. Sizes of the molicules were found to be quite compatible with the sizes of cavities, or channel intersections or pore channels. The insoluble coke was composed of highly polyaromatic molecules partly located in the micropores of zeolite and partly formed an external envelope around the zeolite crystal. The higher coke contents yielded the higher polyaromatic molecules or the insoluble coke.

It was clear that the soluble coke components were too weakly basic to retain adsorbing on the active sites at high reaction temperature. The deactivation therefore should not result from poisoning of the active acid sites but from limitation or blockage of the access of reactants to these sites.

The classification of pore blockage effects on various zeolite pore structures are schematized in Figure 3.18 [101,102]. When the pore system is constituted of non interconnecting channels (A), deactivation occurs through pore blockage, Existence of cages along the channels (B) enhances coke formation, and therefore the zeolite is more rapidly deactivated.

When the pore system is constituted of interconnecting

channels without cavity (C) deactivation occurs initially through (i) limitation of the accessibility to active sites, then (ii) blockage of the sites at the channel intersection in which the coke molecules, are situated. Lastly at high coke content, (iii) coke molecules, located on the outer surface of the crystallite, block the access to the sites in channels in which there are no coke molecules.

When the pore system is constituted of interconnecting cages with large apertures (D) mode of deactivation by coke is almost the same with those with no cages except that the rate of coke formation is higher because of less steric constraints on the reaction(s).

When the pore system comprises cavities with small apertures (E), molecules of coke limit the access to the active sites of the cavities where these molicules are trapped. The deactivation effect of coke of these pore structures, the same as those mono-dimensional pore structures, is very pronounced.

In the case where zeolite contain interconnecting pore structure with primary (larger) channels or cages, P, and secondary (smaller) channels or windows, S. Its aging will be resemble to those of non-interconnecting channels when S is much less than P. The existence of the smaller pore systems will be beneficial for catalysts regeneration.

3.7 General mechanism of coke formation

Coke originates mainly from either olefinic [104,105] or aromatic [102] compounds, Coke from different origins has neither

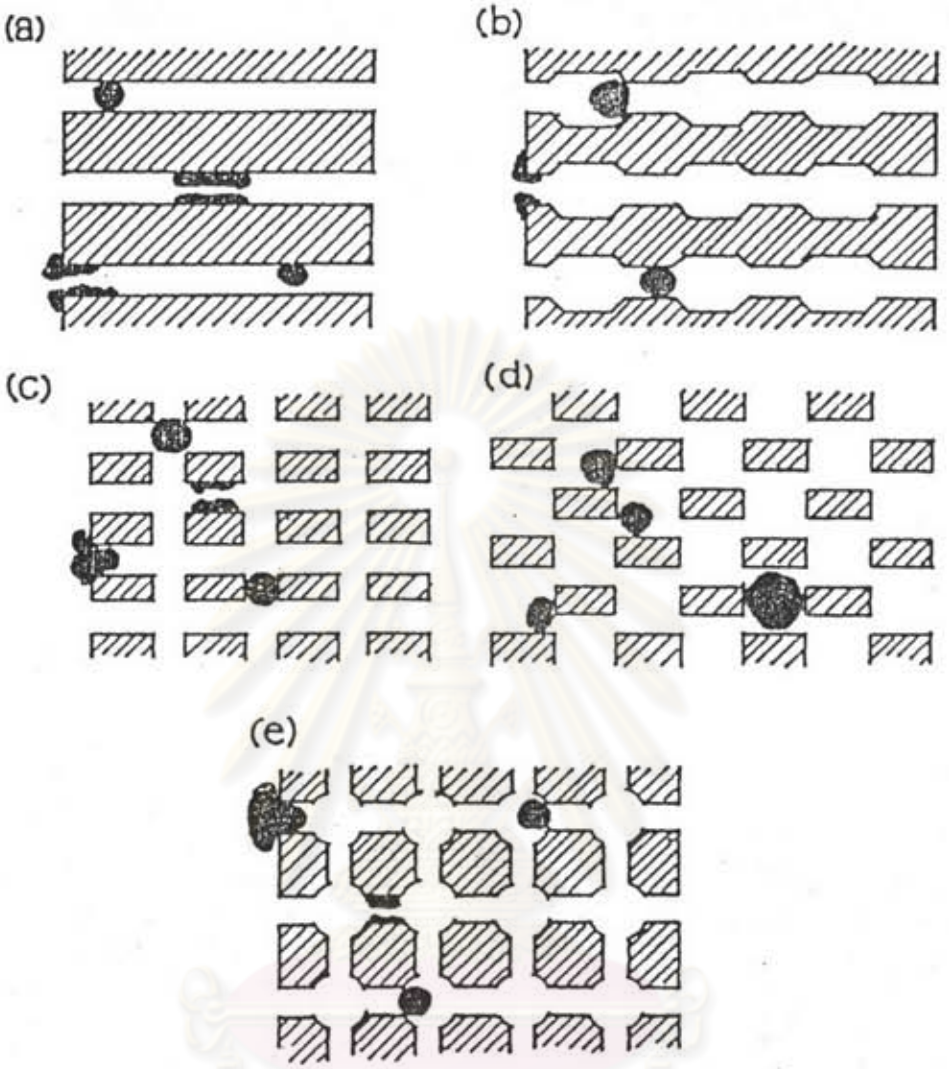

Figure 3.18 Classification of pore blockage effects in zeolites [101].

a) Non-interacting channels (e.g. Mordenite)

b) Non-interconnecting channels with cages (e.g. Offretite)

c) Interconnecting channels without cavities (e.g. ZSM-5)

d) Interconnecting cages with small aperture (e.g. Erionite)

e) Interconnecting cages with large apertures (e.g. Y type)

the same efficiency for its formation nor leading to the same type of deposit. Figure 3.19 depicts the general scheme for the mechanism of coke formation which shows the shape selective constraints in zeolite coking. In small and medium pore zeolites, deposition of pseudo-aromatic coke cannot occur internally. Deactivation may result from deposition of high molecular weight (nearly) linear oligomers if the reaction temperature is too low to induce cracking. Aromatic coke is formed either in large pore zeolites or at the surface of all zeolites.

Figure 3.20 describes possible reaction path ways for consecutive coking (A), and competitive or parallel coking (B) [101]. In both cases, coke formation increases with higher contact time (lower space velocity, higher concentration of active sites, etc.) and decreases when shape selectivity constraints are operative (dashed area). When coke formation is parallel to the main reaction sequence, decreasing contact time (B, 3) always reduces coke and product yields. In contrast, two different situations are met when coking is consecutive. Reducing the contact time at high space velocity (A, 1) also decreases coke and product yields whereas at low space velocity (A, 2) coke is reduced and products are enhanced. Obviously, optimum operating conditions must exist which maximize the product to coke yield ratio.

A remain mechanistic question concerns the nature of the active sites involving in coke formation. It was proposed that the formation of carbonaceous residues proceeded on multi-points adsorption centers, containing more than one Al atom. Coking of high Al content zeolites such as type X or type Y involves with both

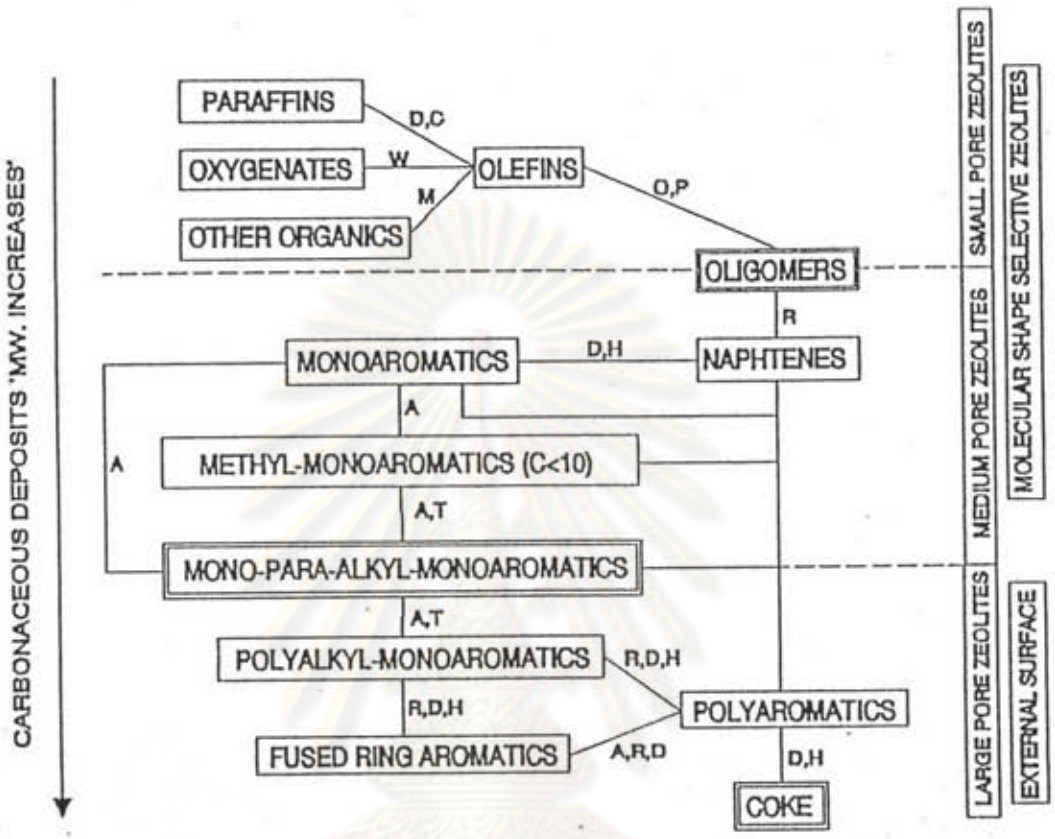

Figure 3.19 Schematic representation of the mechanisms responsible for the formation of carbonaceous deposits [101].

A = Alkylation
C = Cracking
D = Dehydrogenation
H = Hydrogen transfer
M = Miscellaneous
O = Oligomerization
P = Polymerization
R = Cyclization
T = Transalkylation
W = Dehydration

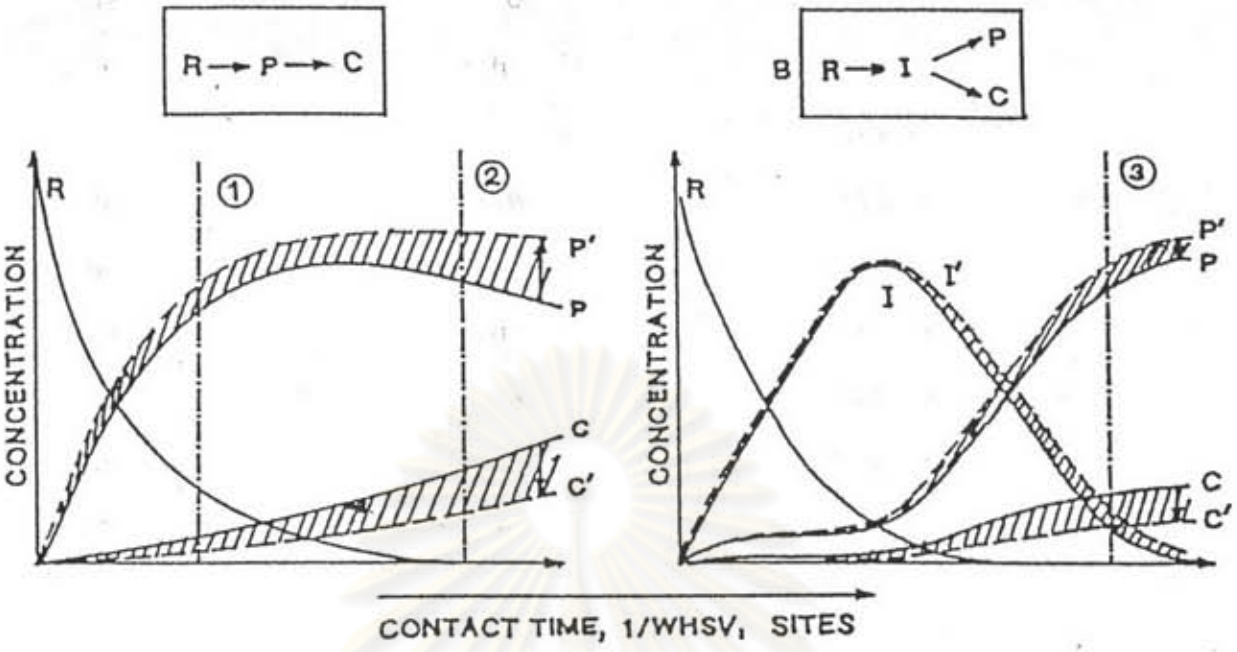

Figure 3.20 Reaction pathways for the formation of products and coke [101].

A = Consecutive coking

B = competitive coking

R = Reactants

C = Coke

Bronsted and Lewis sites. Only the Bronsted sites play the essential role in the coking of high silica zeolites.

Besides yielding higher effective contact time, increasing the number of acid sites enhances the paraffin cracking reaction producing a larger number of olefins and carbonium ions which can eventually contribute to coke. It was expected that aging should increase with Al content. Also, it was found that catalytic sites on coke itself can lead to growth of external coke or reorganization of surface coke deposits.